Multimedia Tools and Applications (2023) 82:38297–38317
https://doi.org/10.1007/s11042-023-14647-z

# A significantly enhanced neural network for handwriting assessment in Parkinson's disease detection

**Aite Zhao**[1] · **Jianbo Li**[2]

Received: 26 May 2021 / Revised: 26 April 2022 / Accepted: 3 February 2023 /
Published online: 25 March 2023


**Abstract**
In recent years, machining learning aided diagnosis can provide non-invasive, low-cost tools to support clinicians and assist the diagnosis and monitoring of neurodegenerative disorders, in particular Parkinson's disease (PD). As an important motor symptom, disorder of the hand motion is usually used for diagnosis and evaluation of PD; moreover, majority of the patients with PD have handwriting abnormalities, which plays a special role in PD detection. In this paper, as an useful tool, we propose a novel hybrid model to learn the handwriting differences between PD patients and healthy controls, by learning and enhancing significant features from three handwriting exams, i.e., meander, circle and spiral. Based on a three-layer convolutional neural network (CNN) and a bidirectional gated recurrent unit (BiGRU), the proposed network can assess the potential of sequential information of handwriting in identifying Parkinsonian symptoms. Compared with several state of the art studies, the recognition rates of our proposed framework are 92.91%, 85.71% and 90.55% respectively in these three tests, which verifies the excellent classification effect.

**Keywords** Machine learning · Hand motion · CNN · BiGRU · Parkinson's disease

## 1 Introduction

Parkinson's disease (PD) is a progressive neurodegenerative disorder, which is characterized by motor symptoms such as tremor, rigidity, slowness of movement and problems with gait [2, 28, 30, 31, 51, 54, 55]. PD often impairs the sufferer's motor skills and causes specific disturbances of hand motor function. Thus, analysis of hand motion parameters is invaluable for better understanding of the mechanisms of movement disorders and the

✉ Jianbo Li
lijianbo@qdu.edu.cn

Aite Zhao
zhaoaite@qdu.edu.cn

[1] School of Business, Qingdao University, Qingdao, China

[2] College of Computer Science and Technology, Qingdao University, Qingdao, China

development of PD. Patients with PD have their own unique hand motion patterns [28, 30]. The characteristics of hand tremor in Parkinson's disease patients are significant tremor in static state, aggravation of tremor in tension or excitement, and alleviation or cessation of tremor in random movement. In addition, the range of hand shaking in PD patients is small, and the typical performance is that the thumb and index finger are "rubbing pills action", which are the potential factors leading to handwriting abnormalities. Therefore, as one of the effective approaches to detect early Parkinson's disease, handwriting is widely applied in clinical diagnosis. Moreover, hand movements of patients with different severity degrees of PD are of various appearances that can be quantified by the unified Parkinson's disease rating scale (UPDRS) and Hoehn & Yahr rating scale (H & Y) [13, 26, 40, 48]. In this paper, we develop a learning model to effectively analyse the handwriting characteristics and identify individual diseases.

Over the years, various dynamic attributes of handwriting, such as pen pressure, stroke speed, in-air time, which can be collected by handwriting acquisition tools, have been evaluated for PD detection. Motion events, and their associated spatio-temporal properties extracted in the handwriting test, enable effective classification of PD patients through the identification of unique sequential patterns [9, 22, 41, 42]. Developing a decision support tool of handwriting classification based on these spatio-temporal information is desirable, as it can provide a non-invasive and low-cost solution to support the standard clinical evaluations carried out by medical experts.

Machine learning are popular approaches for signal and image classification, which have been applied to the classification of sequences such as the speech signal or handwriting text-line images [11, 19, 36]. With regard to the challenging PD diagnosis problem, these methods provide superior specifications. Some examples of such classifiers are decision trees [25], random forest [46], naive Bayes [3], the artificial neural networks (ANN) [5, 24, 44, 49], support vector machines (SVM) [29, 33], the sequential minimal optimization (SMO) method [12], and convolutional neural networks (CNN) [41].

Handwriting evaluation and classification require rich fine-grained features, as differences between handwriting styles are usually much more subtle than those between common hand movement categories. To capture the subtle writing features without losing other key biomarkers, we use three types of handwriting, i.e., spirals, meanders, circled movements to describe multiple hand movement characteristics. The three handwriting images are shown in Fig. 1. It can be distinctly seen that the handwriting of PD patients is disordered and unsmoothed, and there is a big gap compared with the handwriting of healthy people. However, CNN and LSTM can only perform convolution, weighting and other operations for the global, and do not fully consider the local subtle changes [15, 18, 21, 52, 53]. Therefore, we need a learning algorithm that can not only highlight the global features, but also capture the local changes to distinguish the handwriting of PD patients and healthy subjects. The challenges of our research is to learn and detect these dynamic subtle changes.

However, detecting subtle changes is not trivial. For instance, multiple handwriting images differ greatly in contents. We distinguish the handwriting of different participants by calculating the curvature and signal-to-noise ratio (SNR) of the data. We add a weight to the data with larger curvature and smaller SNR to increase the significance of the features so that they can be trained by the neural network. In our system, we design a data preprocessor for image binaryzation and weight calculation, a feature extractor for spatio-temporal feature selection, and then use a decision-making layer to establish a diagnostic model which determines whether the input handwriting samples come from PD or normal people.

Specifically, to highlight unique spatio-temporal characteristics of the ordinal data, we use a feature extractor to undertake feature analysis. It has built-in BiGRU and CNN to

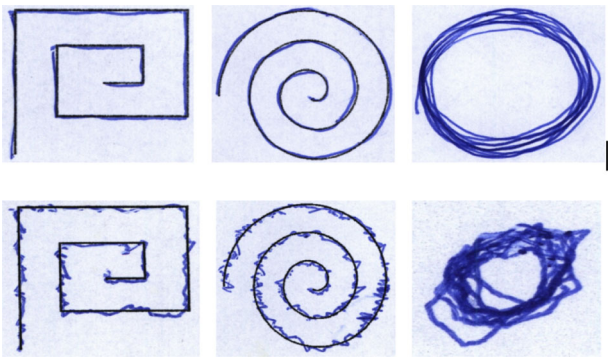

**Fig. 1** The handwriting data used in this project: We evaluate the proposed approach over the NewHandPD dataset, consists of the image data, i.e., spiral, meander, circled movements images

encode the global features by convolutions and gated units over the input data. Afterwards, using the enhanced spatial-temporal features of handwriting data, we expect to construct a decision-making layer (softmax) for PD detection.

The main contributions of our work are summarized as follows:

- A data preprocessor for image binarization and weight calculation is designed, including binarization of original handwritten data, curvature and SNR calculation. Binarization is to remove other interference factors that affect the handwriting images, and the weight calculation of curvature and SNR is to enhance the feature significance of the handwriting of PD patients, so that the separable features can be fed into the feature extractor.
- A feature extractor is constructed to learn the spatio-temporal information of handwritten data, including a set of parallel bidirectional gated recurrent unit (BiGRU) and CNN components. BiGRU has a layer of scalable GRU unit to extract the temporal characteristics of handwritings, and CNN contains three convolution layers to track the spatial changes of handwritings.
- The decision-making layer obtains features from preprocessor, CNN and BiGRU, utilizes series splicing to form fusion features, and determines the final classification result with softmax classifier.
- The proposed hybrid model can selectively enhance the significance of features as well as extract critical spatio-temporal information of handwriting for identifying PD. The proposed method is comprehensively evaluated over three types of PD handwriting exams.

The rest of this paper is organized as follows. Related work is reviewed in Section 2. Section 3 introduces the proposed framework and the details of each module. Section 4 provides the results of the system evaluation. Conclusion is given in Section 5.

## 2 Related work

We here explore state-of-the-art technologies on the recognition of hand movement in Parkinson's disease in the following two areas of interests: traditional classifiers on hand motion recognition of PD, and deep learning methods on hand motion recognition of PD.

### 2.1 Traditional classifiers on hand motion recognition of PD

It is well known that Parkinson's disease biomarkers can be analyzed through various forms of human-computer interaction, including precise grip strength, finger tapping test (FTT), hand and finger movement, and handwriting [3, 10, 16, 25, 29, 33, 46]. Several traditional classifiers can be able to capture the difference between normal and abnormal hand motions, and have been applied in the diagnosis of the PD. Based on the handwriting data, an innovative intelligence model with a combination of a chaos-mapped bat algorithm (CMBA) and a support vector machine (SVM) is introduced for the early-stage identification of PD [33]. Additionally, a model-free computer-assisted handwriting analysis based on a SVM classifier was proposed for representing writing patterns of the PD patients [29]. Giardo et al. utilized the time series analysis of key holding time and support vector machine (SVM) to detect the significant differences between PD patients and the healthy control group, and the subsequent research on the classification characteristics of larger groups obtained 78% accuracy [16]. The above evidence shows that SVM was a popular machine learning method in PD detection. The advantage of SVM was to solve the small sample, nonlinear and high-dimensional regression and binary classification problems. Because the kernel function method overcome the problems of dimension disaster and nonlinear separability, it did not increase the computational complexity when mapping to high-dimensional space. Because SVM classifier was only determined by support vector, it can also effectively avoid over fitting. However, SVM only gave two classification algorithms, while in data mining, it was generally necessary to solve the classification problem of multi classification, while the effect of support vector machine was not ideal. And SVM theory used the fixed penalty coefficient $C$, but the losses caused by the two errors of positive and negative samples were different.

Furthermore, the decision tree also showed its advantage in PD classification, thereby obtaining samples with high separability [23]. Although it can deal with the classification problem of multi-dimensional output, compared with the black box classification model such as neural network, the decision tree can be logically well explained, but the decision tree algorithm was very easy to over fit, resulting in weak generalization ability. The random forest was proposed to differentiate PD patients from healthy controls by using the results of handwritten exams [46, 47]. Each tree in the random forest selected some samples and characteristics to avoid over fitting to a certain extent; However, the random forest will be over fitted in some noisy classification or regression problems. For the data of attributes with different values, the attributes with more values will have a greater impact on the random forest. Principal component analysis (PCA) was applied to quantify the severity of symptoms related to the finger tapping of PD imitators with high accuracy [35]. However, PCA was mainly to eliminate the correlation between variables, and assuming that this correlation was linear, it can not get good results for nonlinear dependence. Besides, an ordinal logistic regression model and a greedy backward algorithm were used to identify the most relevant features in the prediction of MDS-UPDRS [38]. Unfortunately, it was easy to under fit and the classification accuracy was not high. When the data features were missing or the feature space was large, it can not get good performance effect.

However, these studies did not evaluate subtle changes of hand movement disorders, such as the frequency of hand tremor, the change of force in hand movement, and the slight deviation in handwriting test. In this paper, the outputs of different handwriting tests of patients with Parkinson's disease will be considered to comprehensively identify and evaluate the disease status. Benefiting from the feature learning and data computing ability of

deep learning methods, these subtle changes can be easily captured and quantified, which can be used as the basis for the final distinction between PD patients and healthy people.

### 2.2 Deep models on hand motion recognition of PD

Thus, hand motion is quantified into different dimensions of data, for which a variety of deep learning methods are adopted to model its inherent information, and finally evaluated the state of the diseased object.

The handwriting data composed of multiple ordered images including temporal and spatial information. With these temporal data, the long-short term memory (LSTM) [34] has the ability of learning time series to obtain movement information for patients with PD, which can improve the detection sensitivity and analyze the complexity and diversity of the motor behavior objectively. For instance, the application of various deep learning architectures, i.e., the convolutional neural network (CNN) and the bidirectional LSTM (BiLSTM), was investigated to PD detection through time series classification [41]. A novel classification model based on one-dimensional convolutions and bidirectional gated recurrent units (BiGRUs) was proposed to assess the potential of sequential information of handwriting in identifying Parkinsonian symptoms [9]. A multidimensional recurrent neural network (MDRNN) was proposed to deal with high-dimensional data such as videos (3D) or images (2D), and used for handwriting recognition tasks [43]. However, the handwriting characteristics of Parkinson's disease are not obvious, and the details of subtle changes can not be captured only by temporal model or spatial model.

Because the output of the handwriting test has the form of images, CNN is often selected to highlight spatial features [7, 8, 14, 37]. Gazda et al. presented an approach in which end-to-end processing by CNN was utilized to diagnose PD from handwriting images [14]. Another modified CNN model was proposed for recognizing handwritten characters [7]. The CNN architecture ALexNet was used to refine the diagnosis of Parkinson's disease [37]. The above work has obtained more than 80% recognition results. The handwriting of Parkinson's patients and healthy subjects with similar severity can not be successfully analyzed only by CNN model, because the handwriting of patients with mild Parkinson's disease has no obvious hand dyskinesia.

Inspired by the existing advanced methods, this paper reports a hybrid model integrating temporal and spatial to extract and recognize handwritten features of patients with Parkinson's disease, and preprocess the enhanced features of the input image. The model not only avoids the phenomenon of over fitting, but also can successfully analyze and extract the temporal and spatial features of the input image, and distinguish Parkinson's patients from healthy subjects. The experimental results show that the proposed method is superior to the existing state of the art machine learning approaches.

## 3 Proposed methods

In order to achieve successful handwriting recognition for PD patients and healthy people in a less controlled environment, we here propose a hybrid framework, significantly enhanced neural network (SENN), for feature enhancement, extraction and classification. Firstly, we introduce the preprocessor for feature enhancement. Then, we describe the architecture of the feature extractor for spatio-temporal feature extraction, followed by detailed discussion on the individual components. Finally, we introduce the decision-making layer

for distinguishing and scoring the enhanced spatio-temporal features before supplying the final diagnostic result.

### 3.1 The overall framework

Our proposed framework is shown in Fig. 2. In this system, the handwriting data is fed into the preprocessor. The preprocessor consists of binarization, signal to noise ratio (SNR) calculation and curvature calculation to handle the input for enhanced data generation. Afterwards, the binarized image is multiplied by the reciprocal of SNR to highlight the noise (data from the patients). The calculated curvature map is added to form fusion data and input to feature extractor for training. For the feature extraction module, a bidirectional gated recurrent unit (BiGRU) is utilized for analyzing the temporal dynamic changes of the handwriting data, while a three-layer convolutional neural network (CNN) is designed to consider the spacial features of the input data. After having obtained features from the feature extractor, we send the spacial and temporal features to the decision-making layer that can describe different classification outcomes. As shown in Fig. 2, our system is an end-to-end discriminant framework with detection outputs to train the handwriting recognition network.

First, we formulate the problem for handwriting recognition. The image sequences are defined as $X = \{x_i \in \mathbb{R}^{W*H}, i = 1, 2, 3, ..., N\}$ with corresponding 2-class label sequences $L$, $N$ is the sample numbers of the input data, $W$ and $H$ are the width and height of each frame of the image.

### 3.2 Data enhancement

First of all, we binarize all the handwriting images, and the image features are more significant, which are shown in Fig. 3. Compared with Fig. 1, the background of the image data is deleted and only the binarized handwriting is retained.

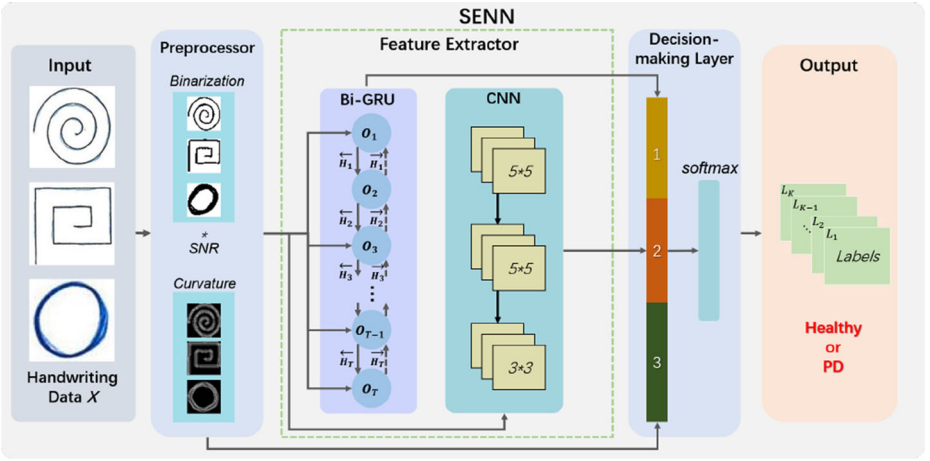


**Fig. 2** The structure of the proposed framework. It includes three modules: a preprocessor for image binarization and weight calculation, a feature extractor for spatio-temporal feature extraction, and a decision-making layer for classification

**Fig. 3** The handwriting data after binarization. Image binarization makes the salient features more obvious and eliminates the background

In this section, curvature is defined by differential according to the rotation rate of the tangent direction angle of a point on the curve to the arc length, indicating the degree of curve deviation from the straight line. The larger the curvature is, the more curved the curve is. For two-dimensional discrete digital images, the following formula can be used to calculate the mean curvature:

$$H = \frac{(1 + U_x^2)U_{yy} - 2U_x U_y U_{xy} + (1 + U_y^2)U_{xx}}{2(1 + U_x^2 + U_y^2)^{\frac{3}{2}}} \tag{1}$$

where $U$ is the input image, $x$ and $y$ are the two-dimensional coordinates of the image, $U_x$ and $U_y$ are the component sets of the input image in two dimensions. Generally, the average curvature is calculated by discretizing the formula. Another method is to avoid discretization by quadric surface fitting:

$$U(x, y) \approx f(x, y) = C_5 x^2 + C_4 y^2 + C_3 xy + C_2 x + C_1 y + C_0 \tag{2}$$

Then the coefficient $C_i$ is determined by the least square method. After that, we substitute $C_i$ into the above formula to get the following result:

$$H \approx \frac{(1 + C_2^2)C_4 - C_2 C_1 C_3 + (1 + C_1^2)C_5}{(1 + C_1^2 + C_2^2)^{\frac{3}{2}}} \tag{3}$$

The image after curvature calculation is shown in Fig. 4.

Additionally, we also calculate the signal-to-noise ratio (SNR) of the image to determine which image is more disordered, so as to highlight the handwriting characteristics of PD patients. The SNR refers to the ratio of normal signal to noise signal. Here we take the original image without handwriting (testing image) as normal signal and the image with handwriting as noise signal. The smaller the calculated SNR is, the greater the noise is, indicating that the test image is more inclined to PD patients. The calculation process of SNR is as follows:

$$SNR = 10 * \log_{10}[\frac{\sum_{x=1}^{N_x}\sum_{y=1}^{N_y}(f(x, y))^2}{\sum_{x=1}^{N_x}\sum_{y=1}^{N_y}(g(x, y))^2}] \tag{4}$$

where $M$ and $N$ are the number of pixels on the height and width of the image respectively, $f(x, y)$ and $g(x, y)$ are the pixel values of the original image and the noise image at the point $(x, y)$ respectively.

And then, we multiply the binary image by SNR, and add the curvature image to get the final fusion feature image as the input of the feature extractor.

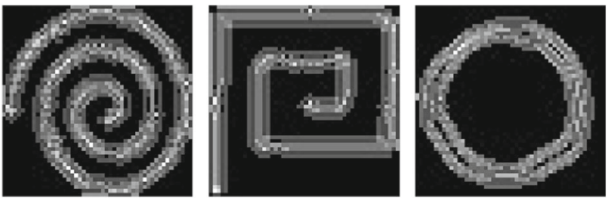

**Fig. 4** The handwriting data after curvature calculation. Calculating curvature can measure the degree of curvature of geometry, which can be used to compare handwriting with different degrees of curvature

### 3.3 The feature extractor

With respect to spatio-temporal feature extraction, we design a network based on the architecture of long short-term memory (LSTM) [17] and convolutional neural network (CNN) [56].

In order to model nonlinear dynamic processes, recurrent neural network (RNN) is widely used to describe temporal dynamic behaviors of time sequences. Long short-term memory (LSTM) is a special form of recurrent neural networks (RNNs) that has been developed to deal with the problem of gradient vanishing and explosion [20]. Different from RNN, LSTM is the basic activation unit at each temporal instant in LSTM. With memory cells and three nonlinear gates (input, forget and output) in the basic LSTM structure, LSTM network is effective in learning long-term temporal dependence since these memory cells can keep their states over long time and regulate the information flows into and out of the cell.

For small handwriting images (we resize the image into 50*50.), we choose the simplest GRU of the gated control mechanism, which is suitable for processing short sequences. Besides, we only use one-layer LSTM, and three internal gated mechanism to encode the data.

The overall architecture of this module is illustrated in Fig. 5. The input data reaches the two components with $T$ time-expanded nodes in BiGRU. As forward LSTM and backward LSTM are combined to form BiLSTM, BiGRU is composed of forward GRU and backward GRU, which can consider the feature inputs of $t + 1$ and $t - 1$ at the same time. Because the output of the forward and backward GRU contains the context information, we take the final output $O_T$ as a part of the fusion feature.

In addition, we also designed a three-layer CNN to analyze the spatial characteristics of the input data, including three convolution layers, i.e. conv1, conv2 and conv3, with 5*5, 5*5 and 3*3 as convolution kernels. Due to the limited size of the input image and the information loss of the pooling layer, we remove the pooling layer in CNN and set only three convolution layers to avoid the loss of more feature details. The output is the second feature in the fusion feature vector.

#### 3.3.1 The GRU cell

Before introducing our model, we will give a brief review of the standard LSTM. In order to model nonlinear dynamic processes, long short-term memory (LSTM) is widely used to describe temporal dynamic behaviors of time sequences [20]. With memory cells and three nonlinear gates (input, forget and output) in the basic LSTM structure, LSTM network is effective in learning long-term temporal dependence since these memory cells can keep their states over long time and regulate the information flows into and out of the cell.

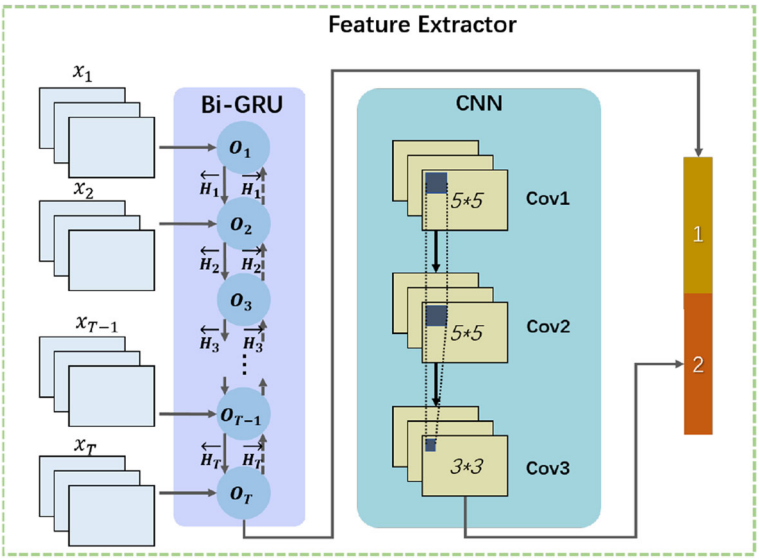


**Fig. 5** The structure of the feature extractor. When we train this model, each memory node of the bidirectional gated recurrent unit (BiGRU) delivers features to calculate the temporal information of context. The convolutional neural network (CNN) includes three layers for spacial feature extraction without pooling

A variant of LSTM, called the gated recurrent unit (GRU), combines the input and the forget gates with an update gate, and mixes the cell and hidden states in each node of the original LSTM, which is used as the learning model [6]. GRU has fewer gates and parameters than the standard LSTM, which helps improving system efficiency to handle a large dataset. Figure 6 shows the structure of a GRU cell and illustrates the operations of the gates. The outputs and inputs in each cell of GRU is described in (5).

$$\begin{cases} z_t = \sigma(W_z \cdot [H_{t-1}, x_t]) \\ r_t = \sigma(W_r \cdot [H_{t-1}, x_t]) \\ \tilde{h}_t = \tanh(W \cdot [r_t \odot H_{t-1}, x_t]) \\ H_t = (1 - z_t) \odot H_{t-1} + z_t \odot \tilde{h}_t \\ O_t = g(W[\overrightarrow{H_t}, \overleftarrow{H_t}] + b) \end{cases} \tag{5}$$

where $x_t$ and $H_t$ are the current input and output of the hidden node at time $t \in \{1, 2, 3..., T\}$. $\sigma$ and $tanh$ are the activation functions. $z_t$ indicates the output of the update gate at time $t$. $r_t$ denotes the reset gate that determines whether or not the previous hidden state is ignored, and $z_t$ is the update gate that determines whether or not the hidden state will be updated with hidden state $\tilde{h}$. The gate structure of the node refers to the internal operation of GRU, which is demonstrated in Fig. 6.

After obtaining the spatio-temporal features, we combine them with the output of preprocessor to get the fusion vectors of three features, and then classify them by softmax classifier to obtain the detection results.

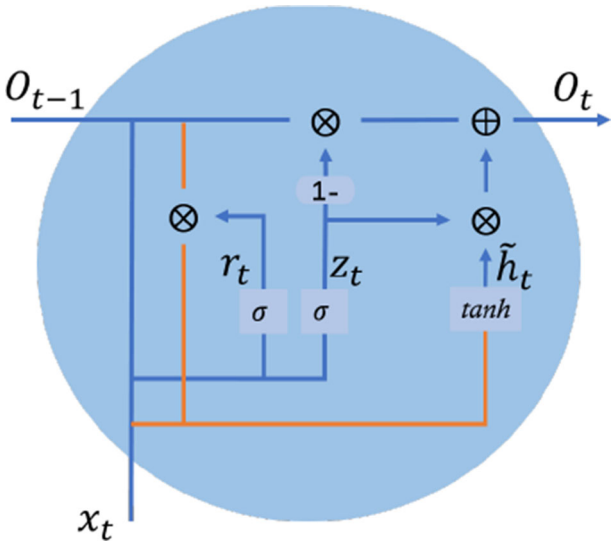


**Fig. 6** The GRU cell. GRU has two gates, a reset gate and an update gate. Intuitively, the reset gate determines how to combine the new input information with the previous memory, and the update gate defines the amount of previous memory saved to the current time step

## 4 Experiments

This section presents our experimental setup and the results of the proposed method, compared against several state of the art methods on a challenging handwriting dataset.

The state of the art technologies compared in this paper include classifiers and deep learning approaches. The classifiers are:

- NB (naive Bayes) is a classification method based on Bayes theorem and independent assumption of feature conditions.
- RF (random forest) is a classifier with multiple decision trees.
- DT (decision tree) refers to a tree structure model which classifies instances based on the tree structure.
- LR (logical regression) is a kind of generalized linear models that use the softmax classification function to generate a multi-classification probability.
- KNN (K-nearest neighbor) is a classifier that finds a $k$ nearest instance and votes to determine the class belonging of the new instance.
- GBDT (gradient boosting decision tree) is an iterative decision tree algorithm, which is composed of multiple decision trees. The results of all the trees are accumulated to determine the final label.

The deep models consist of:

- LSTM (long-short term memory) [34] is a model with expandable nodes, suitable for temporal data.
- BiLSTM (bi-directional long-short term memory) [41] is a combination of forward and backward LSTMs.
- CNN (convolutional neural network) [14] is a kind of feed-forward neural network with a deep structure and convolution calculation.

### 4.1 Dataset specifications

In this section, we give a brief description of the NewHandPD dataset [32] used in our experiment, which is shown in Fig. 1.

The NewHandPD dataset comprises handwritten exams from two groups of individuals: (i) Healthy Group and (ii) Patient Group, being the latter one composed by individuals affected by Parkinson's Disease (PD). The handwritten exams were collected at Botucatu Medical School, São Paulo State University from Brazil.

This dataset is composed of 66 individuals divided in two groups: healthy controls and patients. The first one comprises 35 individuals, as well as the second group contains 31 individuals. Each individual was asked to draw 12 exams, being 4 of them related to spirals, 4 related to meanders, 2 circled movements (one circle in the air and another on the paper), and left and right-handed diadochokinesis. During the exam, there are 9 images for each individual, which means both information can be used to obtain a more descriptive data about each individual. A brief description about each group is as follows:

Healthy Group: 18 male and 17 female individuals with ages ranging from 14 to 79 years old (average age of $44.05 \pm 14.88$ years). Among those individuals, 5 are left handed and 30 are right handed.

Patient Group: 21 male and 10 female individuals with ages ranging from 38 to 78 years old (average age of $57.83 \pm 7.85$ years). Among those individuals, 2 are left handed and 29 are right handed.

Therefore, the NewHandPD dataset is composed of 264 images (104 female and 160 male). The sample ratio of healthy subjects and PD patients is approximately 1:1 (35:31). The number of samples is evenly distributed, and there is no data imbalance. The pixels of the image data obey the uniform distribution, because the sources are the same and have been binarized. The images are labeled in order to provide an easy access to each exam.

### 4.2 Experimental settings

The experiments are conducted with Tensorflow [1] and Python [39] libraries. We will introduce the parameter settings for the three modules: preprocessor, feature extractor and decision-making layer on the handwriting dataset. The average training time of the whole model on the three exams is 8.69min (meander), 5.34min (circle), and 9.81min (spiral). For testing, the mean validation time for achieving the best experimental results of the three modules is 1.45min (preprocessor), 1.89s (feature extractor), 0.62s (decision-making layer), using the system of GTX1050Ti GPU, i5-7300HQ CPU and 8G RAM.

For the handwriting dataset, in the preprocessor, the size of all images is adjusted to 50 * 50 to ensure the consistency of images, then we binarize the images and calculate the SNR and curvature respectively to make the trend characteristics of handwriting more significant. We selected original image as the normal signal, while the image with handwriting as the noisy signal. For normalization, the image is processed into a single channel with the threshold of [0, 255]. In the BiGRU, the normalized data enters in the form of $timestep \times feature\ number$ for each training sample. $timestep$ and $feature\ number$ of the time series are 50 and 50 (the same as the width and height of the image) respectively. In addition, with a learning rate of 0.001 and a batch size of 32, the BiGRU model is trained using a hidden output dimensionality of 128 in each BiGRU node. Values of parameters and hyper-parameters in GRU are determined according to the image size and conventional settings. The output of hidden layer can also be set to other values without affecting the

experimental results. In the decision-making layer, we fuse three features from the former modules, which is classified by a softmax classifier for PD detection.

### 4.3 The results of meander handwriting exam

There are more than 600 handwriting samples in this sub-dataset. Due to the different severity of PD patients, there are early, middle and late stages, the results of meander handwriting exam are also different. For example, the handwriting of some mild patients is similar to that of healthy controls, causing information interference of the classification results.

Meander handwriting exam requires PD patients to draw the results on paper according to the meander like template within an indefinite period of time, using a special pressure sensing pen. Due to the different severity of Parkinson's disease, the handwriting of patients with low severity will be more controlled, and the handwriting will fit the original template better. On the contrary, the handwriting of patients with high severity will deviate from the template because of shaking and other reasons. For healthy people, the handwriting generally does not deviate from the template, unless its writing speed is fast.

The first experiment consists of two comparison groups: PD vs. CO, which shows the difference between healthy people and PD patients. The performance of the proposed model and classifiers is shown in Table 1. In this work, we use 80% of the data for training and 20% for testing. We can see that LR and NB appear over fitting phenomenon, which is not suitable for the meander handwriting data, the effect of these two classifiers can be ignored. In the overall classification, our proposed method performs best, and achieves 92.91% accuracy, surpasses other classifiers. DT and GBDT take the second place. DT training needs less data, while other machine learning models usually need data normalization, such as building dummy variables and removing missing values. Moreover, it can deal with numerical data and classified data, while other techniques can only be used to analyze a certain type of variable dataset. DT can deal with multi-channel output problem.

GBDT has high prediction accuracy on several tasks, and can flexibly deal with nonlinear, and various types of data, including continuous and discrete values. Using some robust loss functions, i.e., Huber and Quantile loss functions, the robustness to outliers is very strong. These advantages shows that the two classifiers are more capable of resolving meander handwriting data.

In the classification of CO and PD, all the classifiers have poor discrimination ability for CO and high discrimination ability for PD, which indicates that the meander handwriting of PD patients is quite different from that of healthy subjects. In the data, the number of samples belonging to PD patients is almost twice that of healthy subjects. In addition, the handwriting of the mild PD patients is similar to that of healthy subjects, which leads to the wrong classification of healthy subjects as PD patients.

Furthermore, the performance of several deep models is illustrated in Table 2. The temporal data processing models BiLSTM and LSTM are stable, CNN achieves similar results of PD and CO, but they still do not surpass the classification results of GBDT, which verifies

**Table 1** Comparison of different classifiers on the meander handwriting exam dataset

| Disease class | DT [23] | GBDT | KNN | LR [38] | RF [46] | NB | SENN |
|---|---|---|---|---|---|---|---|
| CO | 76.09% | 69.57% | 73.91% | 0.00% | 71.74% | 0.00% | 87.23% |
| PD | 90.12% | 96.30% | 81.48% | 100.00% | 90.12% | 100.00% | 96.25% |
| All | 85.04% | 86.61% | 78.74% | 63.78% | 83.46% | 63.78% | 92.91% |

**Table 2** Comparison of different deep models on the meander handwriting exam dataset

| Disease class | LSTM [34] | BiLSTM [41] | CNN [14] | SENN |
|---|---|---|---|---|
| CO | 53.49% | 76.92% | 82.33% | 87.23% |
| PD | 91.67% | 89.77% | 82.35% | 96.25% |
| All | 78.74% | 85.83% | 81.53% | 92.91% |

the superiority of traditional classifiers in this experiment. By comparison, we use the new algorithm of deep learning with information enhancement factor to make the result outperform other deep models. Moreover, in the deep model, LSTM is the most sensitive for PD recognition, with a detection rate of 91.67%, second only to the proposed SENN. However, the average detection rate of LSTM is low, which is affected by CO false detection. Due to the interference of bidirectional scalable unit, BiLSTM successfully avoids the weakness of inaccurate judgment of CO.

The receiver operating characteristic curve (ROC) is also demonstrated in Fig. 7, which illustrates the performance of the proposed model and the learning models. AUC (area under curve) value is calculated as the evaluation criterion, and higher AUC indicates that the model has a stronger classification ability. By comparing the ROC curves, we can see that the top three among the classifiers are our proposed model, GBDT and DT, while BiLSTM outperforms other deep models, achieving the result of 83.35%. When FPR = 0.2, the TPR of the proposed method reaches over 95%, obtaining the fastest convergence result.

### 4.4 The results of circle handwriting exam

The second experiment is designed to separate patients with PD using their circle handwriting patterns for identifying the subtle distinctions of symptoms. Circle drawing does not need template, so it is simpler than meander handwriting test. The circle handwriting

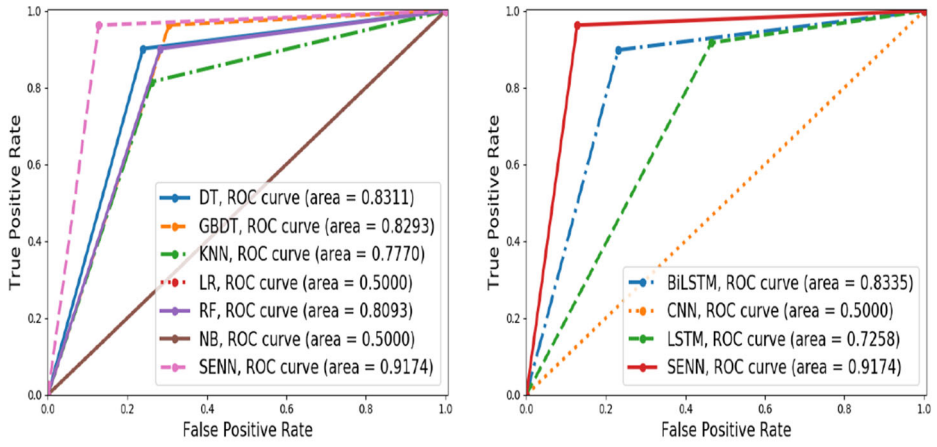


(a) Classifiers (Meander) (b) Deep models (Meander)

**Fig. 7** ROC curves show that the true positive rate (TPR) against the false positive rate (FPR) for the features extracted by different methods: (a) features (Meander) in classifiers; (b) features (Meander) in deep models

smoothness of PD patients is lower, and the noise is larger, which is the reason for designing information enhancement preprocessor.

The second experiment consists of two comparison groups: PD vs. CO, which shows the drawing difference between healthy people and PD patients. The performance of the proposed model and classifiers is shown in Table 3. Following the first experiment, we also select 80% of the data for training and 20% for testing. For the overall classification, our proposed method outperforms other classifiers, achieving 85.71% of the accuracy. KNN ranks the second, which has a training time complexity of $O(n)$. Compared with algorithms such as naive Bayes (NB), the training time complexity has no hypothesis and high accuracy. KNN mainly depends on the limited neighboring samples around, rather than the method of identifying the class domain to determine the category. Therefore, KNN method is more suitable than other methods for the sample set with more overlapping or overlapping class domains.

For the classification of CO and PD, KNN, LR and RF classifiers successfully recognize 85.71% of the testing samples, which is higher than our SENN model. For the classification of the PD, our method ranks the top among those methods, moreover, all testing samples of PD are correctly identified.

Furthermore, the performance of deep models is illustrated in Table 4. The results of LSTM and BiLSTM are consistent, which are superior than that of CNN. In the classification of PD, our model still obtains the best results. It is noteworthy that in this test, the detection rate of SENN for PD is 100%, and the effect exceeds all the compared deep models, which successfully verifies the feasibility of this scheme.

We also validate the performance by ROC in Fig. 8, which illustrates the performance of the proposed model and the learning models. Compared with the AUC value, KNN has higher classification accuracy, and its AUC value is the second large among all the classifiers, showing the stability of the KNN model.

By comparing the ROC curves, we can see that the top one among the classifiers is KNN, while LSTM-based models perform good in deep models, achieving the result of 77.50%. When FPR = 0.2, the TPR of the proposed method reaches 100%, obtaining the fastest convergence result.

### 4.5 The results of spiral handwriting exam

The third experiment is designed to separate patients with PD using their spiral handwriting patterns. The difference between spiral handwriting test and meander handwriting test is that it has the right angle. This kind of test can detect the tiny hand movements of PD patients, who are more difficult to control their own handwriting process.

This experiment also consists of two comparison groups: PD vs. CO, which shows the drawing difference between healthy people and PD patients. The performance of the proposed model and classifiers is shown in Table 5. Following the second experiment, we also select 80% of the data for training and 20% for testing. For the overall classification,

**Table 3** Comparison of different classifiers on the circle handwriting exam dataset

| Disease class | DT [23] | GBDT | KNN | LR [38] | RF [46] | NB | SENN |
|---|---|---|---|---|---|---|---|
| CO | 71.43% | 71.43% | 85.71% | 85.71% | 85.71% | 71.43% | 77.78% |
| PD | 71.43% | 71.43% | 85.71% | 28.57% | 57.14% | 71.43% | 100.00% |
| All | 71.43% | 71.43% | 85.71% | 57.14% | 71.43% | 71.43% | 85.71% |

**Table 4** Comparison of different deep models on the circle handwriting exam dataset

| Disease class | LSTM [34] | BiLSTM [41] | CNN [14] | SENN |
|---|---|---|---|---|
| CO | 80.00% | 80.00% | 100.00% | 77.78% |
| PD | 75.00% | 75.00% | 50.00% | 100.00% |
| All | 78.57% | 78.57% | 77.87% | 85.71% |

our proposed method achieving 90.55% of the accuracy, showing the advantage of feature extraction and data preprocess. GBDT also outperforms other classifiers on this dataset. RF and GBDT are superior to SENN in the recognition of healthy people, and SENN is the best among all the compared methods in the recognition of handwriting of PD patients.

Meanwhile, the performance of deep models is shown in Table 6. In the classification of PD, our model still obtains the best results. The classification results of CO and PD by LSTM are similar, while the classification of CO by BiLSTM is significantly higher than that of PD, which indicates that there is information deviation in BiLSTM's bidirectional information transmission process, resulting in the extracted information more biased to CO samples. Benefiting from the spatial feature extraction of the convolution, the performance of CNN outperforms LSTM-based methods, which is also related to the complexity of the spiral drawing. In this area, the result of SENN is also more balanced.

We also validate the performance by ROC in Fig. 9, which illustrates the performance of the proposed model and the learning models. Compared with the AUC value, GBDT has higher classification accuracy and AUC value, which indicates the high stability and robustness. Comparing the ROC curves, we can see that the top three among the classifiers are SENN, GBDT and RF, and The AUC of CNN is slightly higher than LSTM and BiLSTM, which is consistent with the accuracy ranking. The experimental results of our model are much better than those of other advanced methods.

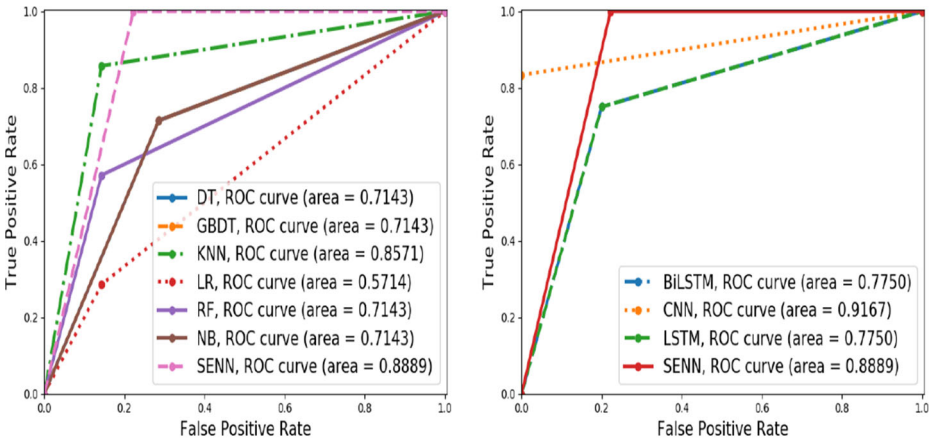


(a) Classifiers (Circle) (b) Deep models (Circle)

**Fig. 8** (a) features (Circle) in classifiers; (b) features (Circle) in deep models

**Table 5** Comparison of different classifiers on the spiral handwriting exam dataset

| Disease class | DT [23] | GBDT | KNN | LR [38] | RF [46] | NB | SENN |
|---|---|---|---|---|---|---|---|
| CO | 78.57% | 96.15% | 85.71% | 100.00% | 97.44% | 100.00% | 95.35% |
| PD | 79.07% | 73.47% | 62.79% | 0.00% | 61.22% | 0.00% | 80.49% |
| All | 78.74% | 87.40% | 77.95% | 66.14% | 83.46% | 66.14% | 90.55% |

### 4.6 Performance of the entire model

In this section, we focus on investigating the effect of the method described in Section 3. Figure 10 demonstrates the recognition accuracy of the testing process by the hybrid SENN. Compared with the three confusion matrices, for Parkinson's disease, the highest recognition rate is in the circle handwriting test, followed by meander and spiral, just in line with the logical order from simple to complex. Experimental results show that the average probability of the proposed model is 92.25%, which can be used in the identification of handwriting test for patients with Parkinson's disease.

Moreover, with the help of the t-distributed stochastic neighbor embedding (t-SNE) visualization method, the classification ability of our proposed method is shown in Fig. 11. We can see that the extracted features after dimensionality reduction have very few errors. In these three experiments, meander and spiral test have more samples, the features extracted by our model are close to linear distribution after dimensionality reduction, and the overlapping samples (misclassified samples) are less. In circle test, the color and classification labels are fully recognized without overlapping. After analyzing the characteristics of these misclassified samples, it is proved that they are similar to the manifestations of non similar samples. Therefore, our proposed SENN algorithm is effective.

In order to solve the overlapping problem, we explore the related work of evaluating image similarity. Although there is no experiment to compare the data similarity on the dataset in this paper, it can be discussed by analogy with the image similarity evaluation method. Traditional visual similarity evaluation indicators include SSIM (structural similarity), MSE (mean square error) and PSNR (peak signal to noise ratio). Because these methods are limited to directly calculating the image distance, the methods of similarity comparison using deep learning methods have gradually increased in recent years. The method of image similarity calculation using deep learning mainly uses the network of deep learning to extract image features, the traditional methods are mostly used to calculate the similarity and distance: 1. Image similarity discrimination based on 2-channel network [50] 2. Deep learning binary hash code for fast image retrieval [27] 3. Learning combinatorial embedding networks for deep graph matching [45]. In addition, we also investigate the objective evaluation method of repaired images based on saliency map features [4], in which the similarity evaluation method is worthy of reference.

**Table 6** Comparison of different deep models on the spiral handwriting exam dataset

| Disease class | LSTM [34] | BiLSTM [41] | CNN [14] | SENN |
|---|---|---|---|---|
| CO | 82.61% | 93.42% | 93.33% | 95.35% |
| PD | 82.86% | 68.63% | 73.08% | 80.49% |
| All | 82.68% | 83.46% | 85.04% | 90.55% |

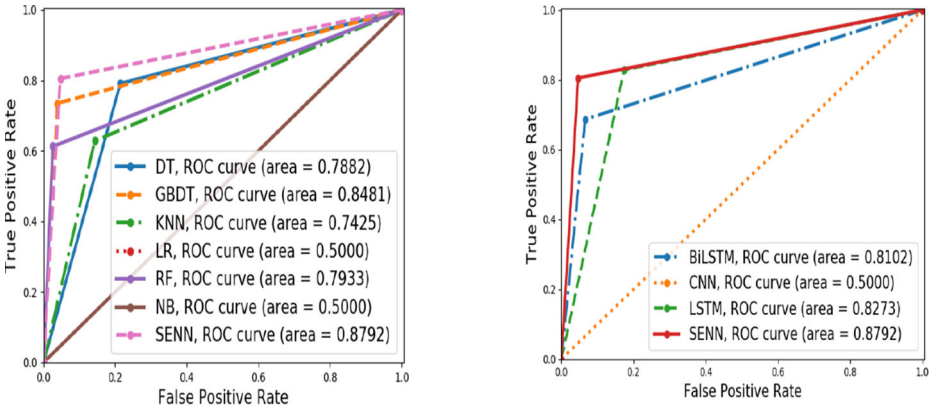


(a) Classifiers (Spiral) (b) Deep models (Spiral)

**Fig. 9** (a) features (Spiral) in classifiers; (b) features (Spiral) in deep models

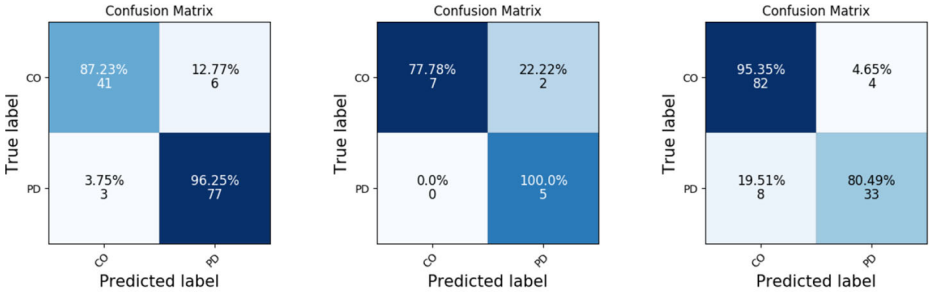


(a) Meander (b) Circle (c) Spiral

**Fig. 10** Confusion matrix for SENN. (a):Confusion matrix of meander handwriting classification;(b):Confusion matrix of circle handwriting classification;(c):Confusion matrix of spiral handwriting classification

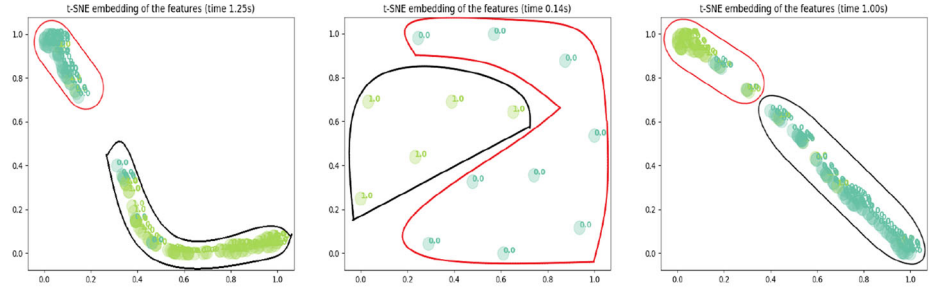


(a) Meander Handwriting Exam. (b) Circle Handwriting Exam. (c) Spiral Handwriting Exam.

**Fig. 11** Comparison of t-SNE feature dimensionality reduction on the handwriting dataset. Sub-figures (a) (b) and (c) represent the feature extracted from our model has been applied on the handwriting dataset

**Table 7** Comparison of different methods on MNIST dataset

| Methods | DT [23] | GBDT | KNN | LR [38] | RF [46] |
|---|---|---|---|---|---|
| Acc | 84.67% | 96.29% | 98.22% | 97.85% | 99.04% |
| Methods | NB | LSTM [34] | BiLSTM [41] | CNN [14] | SENN |
| Acc | 86.03% | 98.33% | 99.23% | 98.93% | 99.78% |

As an extension, we have experimented the method mentioned in this paper on the traditional handwritten digital dataset MNIST. MNIST is a handwritten image dataset containing numbers 0-9. The image has been normalized to an image of 28 * 28 specification. MNIST consists of two parts: training set and testing set. Training set: 60000 handwritten images and corresponding labels, and testing set: 10000 handwritten images and corresponding labels. The experimental results are shown in Table 7. By comparison, other methods have a recognition rate of more than 90% except DT and NB, which verifies the good performance of the algorithm on this public data set. Our proposed SENN achieves 99.78% accuracy and ranks first, marking the superiority of the fusion model. The RF in classifiers and the BiLSTM in deep models have outstanding effects. They are not only suitable for the PD handwriting small sample dataset in this paper, but also stand out on the public large dataset MNIST, indicating its portability and stability. PD handwriting recognition in this paper is also inspired by the process of handwritten digital recognition. Therefore, we have also carried out experiments on the MNIST.

## 5 Conclusion

This paper has presented a novel learning framework for detecting Parkinson's disease, based on human handwriting images. The constituting components in the proposed model delivers individual functionalities, e.g. the preprocessor was used to highlight the linear handwriting data and to encode them as fused images. BiGRU and CNN helped us to conduct feature extraction of the input and achieve spatio-temporal feature of the fused data. The decision-making layer distinguishes each category of the fused features to achieve satisfactory classification. Experimental results have shown that, compared with the other established methods, our proposed model resulted in better discriminative results of PD in an end-to-end form. Through the recognition process in these three exams, we can see that the result of meander handwriting exam is the best, and the number of samples is relatively large. In the future, we can increase the amount of image data of handwritings, which will help to improve the classification accuracy of the designed deep learning model.

**Acknowledgements** This research was supported in part by National Key Research and Development Plan Key Special Projects under Grant No. 2018YFB2100303, Shandong Province colleges and universities youth innovation technology plan innovation team project under Grant No. 2020KJN011, Shandong Provincial Natural Science Foundation under Grant No. ZR2020MF060, Program for Innovative Postdoctoral Talents in Shandong Province under Grant No. 40618030001, National Natural Science Foundation of China under Grant No. 61802216, and Postdoctoral Science Foundation of China under Grant No.2018M642613, National Natural Science Foundation of China under Grant No. 62106117, and Natural Science Foundation of Shandong Province under Grant No.ZR2021QF084.

## Declarations

**Conflict of Interests** We declare that we have no financial and personal relationships with other people or organizations that can inappropriately influence our work, there is no professional or other personal interest of any nature or kind in any product, service and/or company that could be construed as influencing the position presented in, or the review of, the manuscript entitled, "A Significantly Enhanced Neural Network for Handwriting Assessment for Parkinson's Disease Detection".

## References


1. Abadi M, Barham P, Chen J, Chen Z, Davis A, Dean J, Devin M, Ghemawat S, Irving G, Isard M et al (2016) Tensorflow: a system for large-scale machine learning. In: 12Th {USENIX} symposium on operating systems design and implementation ({OSDI} 16), pp 265–283
2. Achanta Sdm, Karthikeyan T, Vinoth Kanna R (2021) Gait-based person fall prediction using deep learning approach. Soft Comput, 1–9
3. Ali L, Khan SU, Arshad M, Ali S, Anwar M (2019) A multi-model framework for evaluating type of speech samples having complementary information about parkinson's disease. In: 2019 International conference on electrical, communication, and computer engineering (ICECCE)
4. Amirkhani D, Bastanfard A (2021) An objective method to evaluate exemplar-based inpainted images quality using jaccardindex. Multimed Tools Appl 80(17):26199–26212
5. Bevilacqua V, Loconsole C, Brunetti A, Cascarano GD, Sciascio ED (2018) A model-free computer-assisted handwriting analysis exploiting optimal topology ANNs on biometric signals in parkinson's disease. Intelligent Computing Theories and Application
6. Che Z, Purushotham S, Cho K, Sontag D, Liu Y (2018) Recurrent neural networks for multivariate time series with missing values. Sci Rep 8(1):60–85
7. Darmatasia, Fanany MI (2017) Handwriting recognition on form document using convolutional neural network and support vector machines (cnn-svm). In: 2017 5Th international conference on information and communication technology (ICoIC7)
8. Deharab ED, Ghaderyan P (2022) Graphical representation and variability quantification of handwriting signals: New tools for parkinson's disease detection. Biocybernetics and Biomedical Engineering
9. Diaz M, Moetesum M, Siddiqi I, Vessio G (2020) Sequence-based dynamic handwriting analysis for parkinson's disease detection with one-dimensional convolutions and bigrus. Expert Systems with Applications
10. Diaz M, Moetesum M, Siddiqi I, Vessio G (2021) Sequence-based dynamic handwriting analysis for parkinson's disease detection with one-dimensional convolutions and bigrus. Expert Syst Appl 168:114405
11. Drotár P, Mekyska J, Rektorová I, Masarová L, Smékal Z, Faundez-Zanuy M (2016) Evaluation of handwriting kinematics and pressure for differential diagnosis of parkinson's disease. Artif Intell Med 67:39–46
12. Durga P, Jebakumari S, Shanthi D (2016) Diagnosis and classification of parkinsons disease using data mining techniques. Int J Adv Res Trends Eng Technol (IJARTET) 3:86–90
13. Evers Ljw, Krijthe JH, Meinders MJ, Bloem BR, Heskes TM (2019) Measuring parkinson's disease over time: The real-world within-subject reliability of the mds-updrs. Mov Disord 34:1–16
14. Gazda M, Hire M, Drotar P (2021) Multiple-fine-tuned convolutional neural networks for parkinson's disease diagnosis from offline handwriting. IEEE Transactions on Systems Man and Cybernetics
15. Gholamalinezhad H, Khosravi H (2020) Pooling methods in deep neural networks, a review. arXiv:2009.07485
16. Giancardo L, Sánchez-Ferro A, Arroyo-Gallego T, Butterworth I, Mendoza CS, Montero P, Matarazzo M, Obeso JA, Gray ML, Estépar RSJ (2016) Computer keyboard interaction as an indicator of early parkinson's disease. Sci Rep 6(10):1–10
17. Greff K, Srivastava RK, Koutník J, Steunebrink BR, Schmidhuber J (2017) Lstm: a search space odyssey. IEEE Transactions on Neural Networks and Learning Systems
18. Greff K, Srivastava RK, Koutník J, Steunebrink BR, Schmidhuber J (2017) Lstm: a search space odyssey. IEEE Trans Neural Netw Learn Syst pubMedId:27411231
19. Hajihashemi V, Ameri Mma, Gharahbagh AA, Bastanfard A (2020) A pattern recognition based holographic graph neuron for persian alphabet recognition. In: 2020 International conference on machine vision and image processing (MVIP)
20. Hochreiter S, Schmidhuber J (1997) Long short-term memory. Neural Comput 9(8):1735–1780

21. Jiang Z, Zhou F, Zhao A, Li X, Li L, Tao D, Li X, Zhou H (2021) Multi-view mouse social behaviour recognition with deep graphic model. IEEE Trans Image Process PP:1–1. 05
22. Kaur S, Aggarwal H, Rani R (2020) Diagnosis of parkinson's disease using deep cnn with transfer learning and data augmentation. Multimedia Tools and Applications, 1–27
23. Lamba R, Gulati T, Al-Dhlan KA, Jain A (2021) A systematic approach to diagnose parkinson's disease through kinematic features extracted from handwritten drawings. J Reliable Intell Environ 7(3):253–262
24. Li F, Ge R, Zhou H, Wang Y, Liu Z, Yu X (2020) Tesia: a trusted efficient service evaluation model in internet of things based on improved aggregation signature. Concurrency and Computation: Practice and Experience
25. Li Y, Yang L, Wang P, Zhang C, Xiao J, Zhang Y, Qiu M (2017) Classification of parkinson's disease by decision tree based instance selection and ensemble learning algorithms. Journal of Medical Imaging & Health Informatics 7(2)
26. Lin G, Wei JI (2019) Research on parkinson updrs prediction model based on gbdt. Comput Technol Dev 29:216–220
27. Lin K, Yang HF, Hsiao JH, Chen CS (2015) Deep learning of binary hash codes for fast image retrieval. In: IEEE Conference on computer vision & pattern recognition workshops
28. Listed N (2013) Neuroscience: my life with parkinson's. Nature 503(7474):29–30
29. Loconsole C, Cascarano GD, Lattarulo A, Brunetti A, Sciascio ED (2018) A comparison between ann and svm classifiers for parkinson's disease by using a model-free computer-assisted handwriting analysis based on biometric signals. In: 2018 International joint conference on neural networks (IJCNN)
30. Meoni S, Macerollo A, Moro E (2020) Sex differences in movement disorders. Nat Rev Neurol 16: 84–96
31. Murthy Achanta SD, Karthikeyan T, Vinoth Kanna R (2021) Wearable sensor based acoustic gait analysis using phase transition-based optimization algorithm on iot. Int J Speech Technol 1–11
32. Pereira CR, Weber SAT, Hook C, Rosa GH, Papa JP (2016) Deep learning-aided parkinson's disease diagnosis from handwritten dynamics. In: 2016 29Th SIBGRAPI conference on graphics, patterns and images (SIBGRAPI), pp 340–346
33. Sahu B, Mohanty SN (2021) Cmba-svm: a clinical approach for parkinson disease diagnosis. Int J Inf Technol 1(73)
34. Sainath TN, Senior AW, Vinyals O, Sak H (2015) Convolutional, long short-term memory, fully connected deep neural networks. In: 2015 IEEE International Conference on Acoustics, Speech and Signal Processing (ICASSP)
35. Sano Y, Kandori A, Shima K, Yamaguchi Y, Tsuji T, Noda M, Higashikawa F, Yokoe M, Sakoda S (2016) Quantifying parkinson's disease finger-tapping severity by extracting and synthesizing finger motion properties. Med Biol Eng Comput 54(6):953–965
36. Senturk ZK (2020) Early diagnosis of parkinson's disease using machine learning algorithms. Med Hypotheses 138:109603
37. Shubhangi DC, Gundagurti P (2020) Deep learning based diagnosis of parkinson's disease using cnn. Int J Sci Res Comput Sci Eng Inf Technol 351–355
38. Stamatakis J, Ambroise J, Crémers J, Sharei H, Delvaux V, Macq B, Garraux G (2013) Finger tapping clinimetric score prediction in parkinson's disease using low-cost accelerometers. Comput Intell Neurosci 2013(2):1–10
39. Swami A, Jain R (2013) Scikit-learn: machine learning in python. J Mach Learn Res 12(10):2825–2830
40. Taleb C, Khachab M, Mokbel C, Likforman-Sulem L (2018) A reliable method to predict parkinson's disease stage and progression based on handwriting and re-sampling approaches. In: 2018 IEEE 2Nd international workshop on arabic and derived script analysis and recognition (ASAR), pp 7–12
41. Taleb C, Likforman-Sulem L, Mokbel C, Khachab M (2020) Detection of parkinson's disease from handwriting using deep learning: a comparative study. Evol Intell 1(1)
42. Tripathi A, Kopparapu SK (2021) Cnn based parkinson's disease assessment using empirical mode decomposition. In: Proceedings of the CIKM 2020 Workshops, October 19-20, Galway, Ireland
43. Voigtlaender P, Doetsch P, Ney H (2017) Handwriting recognition with large multidimensional long short-term memory recurrent neural networks. In: 2016 15Th international conference on frontiers in handwriting recognition (ICFHR)
44. Wang Y, Dong X, Li G, Dong J, Yu H (2021) Cascade regression-based face frontalization for dynamic facial expression analysis. Cogn Comput 99(3)
45. Wang R, Yan J, Yang X (2019) Learning combinatorial embedding networks for deep graph matching. In: IEEE International conference on computer vision
46. Xu S, Pan Z (2020) A novel ensemble of random forest for assisting diagnosis of parkinson's disease on small handwritten dynamics dataset. Int J Med Inf 144:104–283

47. Xu S, Zhu Z, Pan Z (2020) A cascade ensemble learning model for parkinson's disease diagnosis using handwritten sensor signals. J Phys: Conf Ser 1631(1):1–10
48. Yin D, Zhao Y, Wang Y, Zhao W, Hu X (2020) Auxiliary diagnosis of heterogeneous data of parkinson's disease based on improved convolution neural network. Multimed Tools Appl 79(1)
49. Yu X, Li F, Li T, Wu N, Zhou H (2020) Trust-based secure directed diffusion routing protocol in wsn. J Ambient Intell Humanized Comput 99(5):1–13
50. Zagoruyko S, Komodakis N (2018) Learning to compare image patches via convolutional neural networks. arXiv:abs/1504.03641
51. Zhao A, Dong J, Li J, Qi L, Zhou H (2022) Associated spatio-temporal capsule network for gait recognition. IEEE Trans Multimed 24:846–860
52. Zhao A, Dong J, Zhou H (2020) Self-supervised learning from multi-sensor data for sleep recognition. IEEE Access PP(99):1–15
53. Zhao A, Li J, Ahmed M (2020) Spidernet: a spiderweb graph neural network for multi-view gait recognition. Knowl-Based Syst, 206
54. Zhao A, Li J, Dong J, Qi L, Zhang Q, Li N, Wang X, Zhou H (2021) Multimodal gait recognition for neurodegenerative diseases. IEEE Trans Cybernet 9(52):9439–9453
55. Zhao A, Qi L, Dong J, Yu H (2018) Dual channel lstm based multi-feature extraction in gait for diagnosis of neurodegenerative diseases. Knowl-Based Syst 145:91–97
56. Zhao A, Qi L, Li J, Dong J, Yu H (2018) A hybrid spatio-temporal model for detection and severity rating of parkinson's disease from gait data. Neurocomputing 315(NOV.13):1–8